Nanoscale

Accepted Manuscript

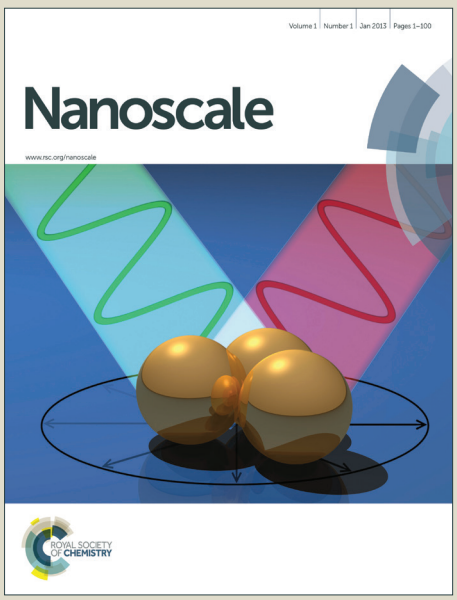

ROYAL SOCIETY OF CHEMISTRY

www.rsc.org/nanoscale

Nanoscale

RSCPublishing

ARTICLE

Bacterial Adhesion Force Quantification by Fluidic Force Microscopy

Cite this: DOI: 10.1039/xoxxooooox

Eva Potthoff[a], Dario Ossola[b], Tomaso Zambelli[b]*, Julia A. Vorholt[a]*

Received 04th November 2014,
Accepted 00th January 2012

DOI: 10.1039/xoxxooooox

www.rsc.org/

Quantification of detachment forces between bacteria and substrates facilitates the understanding of the bacterial adhesion process that affects cell physiology and survival. Here, we present a method that allows for serial, single bacterial cell force spectroscopy by combining the force control of atomic force microscopy with microfluidics. Reversible bacterial cell immobilization under physiological conditions on the pyramidal tip of a microchanneled cantilever is achieved by underpressure. Using the fluidic force microscopy technology (FluidFM), we achieve immobilization forces greater than those of state-of-the-art cell-cantilever binding as demonstrated by the detachment of *Escherichia coli* from polydopamine with recorded forces between 4 and 8 nN for many cells. The contact time and setpoint dependence of the adhesion forces of *E. coli* and *Streptococcus pyogenes*, as well as the sequential detachment of bacteria out of a chain, are shown, revealing distinct force patterns in the detachment curves. This study demonstrates the potential of the FluidFM technology for quantitative bacterial adhesion measurements of cell-substrate and cell-cell interactions that are relevant in biofilms and infection biology.

1. Introduction

The adhesion to surfaces as well as cell-cell interactions are major characteristics of bacterial lifestyles that affect cell physiology, viability, and metabolic activity.[1-3] Initiated by single-cell adhesion, microbial communities are formed in biofilms, which constitute adhesive three-dimensional structures of cells embedded in extracellular polymeric substances attached to surfaces.[2] Bacterial adhesion can be divided into a long-range regime related to nonspecific interactions such as hydrophobic and charged interactions, which are often responsible for the initial contact at separation distances larger than 50 nm, and a short-range regime related to specific receptor-ligand interactions, which occur at distances up to 15 nm.[4, 5] A combination of many different types of interaction between a substrate and the cell wall and cell appendages, such as pili or fimbriae are involved in the adhesion process.[4, 6]: Long-range interactions, which are often mediated by cell appendages, allow the cell to come into close contact with the substrate; at this distance short-range interactions become more important.[2] Thus far, several traditional approaches that investigated the phenomenon of bacterial adhesion provided average data on microbial populations, but lacked information on the single cell level. Those bulk experiments, such as washing assays and flow chamber or spinning disk approaches, yielded semi-quantitative data on the adhesion behavior of bacterial populations.[7, 8] Later, quantitative force measurements on the single cell level were achieved by single-cell force spectroscopy (SCFS) using atomic force microscopy.[9-11] Initially invented for high-resolution imaging, atomic force microscope (AFM) rapidly showed potential for quantifying interaction forces.[7, 12-14] Here, a cantilever acts as a spring, and its bending, which correlates with tip-surface interactions, is recorded via a laser that is reflected from the cantilever onto a photodiode. Knowing the spring constant of the cantilever enables the conversion of the cantilever deflection into interaction forces. The possibility to perform measurements in liquids facilitates the force measurements between living cells and even single molecules under physiological conditions.[15, 16] In conventional SCFS, a bacterium is irreversibly attached to a tipless cantilever[17-19] or a pyramid[20] or sphere shaped tip,[21] resulting in a "cell probe", i.e., one cantilever with one cell. This “cell probe” is then brought into contact with the substrate at a defined force setpoint for a chosen contact time and then retracted. Chemical, irreversible cell immobilization on the cantilever limits biological replicate measurements in SCFS because of the long time required to perform a statistically significant number of measurements due to the labor-intensive immobilization and calibration procedure; this requirement likely explains why in the majority of published studies only a limited number of cells were measured.[18, 21] Coating the cantilever to generate specific

receptor-ligand, electrostatic[18], or hydrophobic- interactions[20] or using commercially available glue or bioinspired wet adhesives[22] often does not provide sufficient strength to withstand the cell-substrate interaction forces: the cell is often detached from the cantilever instead of the substrate during retraction of the cell probe. Fluidic force microscopy (FluidFM) provided an unprecedented immobilization protocol that combines the precise force control of a conventional AFM with a microfluidic system.[23, 24] More precisely, a hollow cantilever with a defined opening at the end is connected to a pressure controller. Applying underpressure results in cell immobilization on the cantilever aperture, whereas overpressure application leads to cell release from the cantilever. The FluidFM is placed on top of an inverted fluorescence microscope to visualize and control all experimental steps. FluidFM circumvents the problems of irreversible, time-consuming, chemical-based cell fixation to the cantilever. Instead, it introduces reversible cell immobilization (Figure 1 A, Figure 2 A),[25, 26] which is important for measuring the substrate attachment of many individual cells at higher throughput, and thus allows for the generation of data on cell-to-cell variations. Although FluidFM has already been established to measure the adhesion forces of yeast and mammalian cells,[25] here, we adapted the tip design and protocols to apply FluidFM-based SCFS to recordings of adhesion forces of single bacterial cells. Specifically adapted FluidFM protocols for short- and long-term adhesion measurements were implemented for morphologically different bacterial species and were validated using the Gram negative rod-shaped model microorganism *Escherichia coli* and the clinically relevant spherical *Streptococcus pyogenes* growing in chains.[27]

2. Experimental details

Culture conditions

E. coli expressing gfp-mut[44] were grown in Luria-Bertani medium (10 g of tryptone, 5 g of yeast extract and 10 g NaCl in 1 liter of distilled water). Overnight cultures were diluted 10 times and incubated at 37 °C and 180 rpm until they reached an OD_{600} of 0.4.

The isogenic *S. pyogenes* knock out mutant lacking the M protein[45] was grown in Todd–Hewitt broth (BD) supplemented with 2% yeast extract (THY, Oxoid, Pratteln, Switzerland) at 37 °C without shaking and with the expression of GFP on a pDCerm-derived plasmid in the presence of 5 μg ml^{-1} erythromycin.

Prior to the force spectroscopy experiments, cultures were washed three times as follows. A 1-ml aliquot of the cultures was pelleted at 12,500 rpm (Eppendorf centrifuge 5424) for 1.5 min at room temperature and was subsequently resuspended in 1 ml of filtered (0.22 mm pore size) phosphate-buffered saline (PBS: 8 g of NaCl (Merck), 0.2 g of KCl, 1.44 g of Na_2HPO4 and 0.24 g of KH_2PO_4 (all from Fluka) in 1 L of distilled water, pH 7.4).[46] Afterwards, the cell numbers in the glass dish (WillCo Wells B.V., The Netherlands) in which the force spectroscopy experiments were finally performed were adjusted to obtain an OD_{600} of 0.001 in 4ml PBS.

Substrate preparation

50-mm glass dishes (WillCo Wells B.V., The Netherlands) were sonicated in ultra-pure water and 2-propanol (Scharlau, Spain) for 10 min at room temperature in a Branson 2210 Ultrasound bath, dried under flowing nitrogen gas and plasma cleaned (Plasma Cleaner PDG-32G, Harrick Plasma, USA) for 2 min immediately prior to the coating procedure. For polydopamine (PDA) coating of the substrate, clean glass dishes were immersed in a 10 mM TRIS HCL solution, pH 8 containing 4 mg ml^{-1} PDA (Sigma) for 1 hour, then intensively washed with filtered PBS and dried with N_2. For poly-L-lysine (PLL) coating, a 0.5 mg ml^{-1} PLL solution was prepared in filtered ultra-pure water. Glass dishes were immersed in that solution for 45 minutes and subsequently extensively rinsed with filtered PBS. For bacteria-glass interaction measurements, glass dishes were used after cleaning with 2-propanol and ultra-pure water as described above.

Cantilever preparation and calibration

Rectangular, hollow silicon nitride cantilevers carrying a hollow pyramid at their free-end were chosen for bacterial adhesion measurements (Cytosurge AG, Switzerland). The cantilevers were 36 μm wide and 150 μm long and had a channel height of 0.2 or 1 μm, resulting in a stiffness of approximately 0.2 or 2.5 N m^{-1}, respectively. Before scanning electron microscopy (SEM) imaging and FIB milling of the cantilever at SCOPEM at ETH Zürich, a thin (10-20 nm), amorphous carbon layer was sputtered on the probe to limit charging effects. The coating was removed by a 2-minute O2-plasma treatment afterwards. The pyramid apex of the closed pyramidal probes was sloped to compensate for the 10° tilt angle of the AFM probe holder. Subsequently, circular openings with diameters ranging from 300 to 900 nm were milled perpendicular to the flattened pyramidal apex using FIB. Consequently, defined openings parallel to the substrate were achieved. For the hemi-cylindrical pyramidal opening, pyramid apexes were also flattened with a 10° angle with respect to the cantilever. Then, from the same angulation, cylindrical apertures with a diameter of 600 nm (longitudinally) centered on the flattened apex plane were milled to achieve the desired opening and hemi-cylinder radius.

Prior to all experiments, the probes were plasma-cleaned for 30 s (Plasma Cleaner PDG-32G, Harrick Plasma, USA) and covered with an antifouling coating of 0.5 mg ml^{-1} PLL (20 kDa) grafted with poly-ethylene glycol (PEG) (2 kDa) (PLL-*g*-PEG) (Surface Solution SuSoS AG, Switzerland) in filtered ultra-pure water. The positively charged PLL backbone is spontaneously attracted to negatively charged surfaces while the bound, protruding brush-like PEG chains diminish unspecific cell binding without affecting cell viability. [25, 47] FluidFM probes were coated from the in- and outside with PLL-*g*-PEG for 1 hour and subsequently washed in filtered

PBS for 5 min. [25, 47] The cantilever sensitivity was calibrated using software-implemented scripts based on the formalism described by Sader et al. [48]

SCFS procedures using FluidFM

A FluidFM connected to a pressure controller (Cytosurge AG, Zürich and Nanosurf AG, Liestal, Switzerland) was mounted on an Axio Observer D1 inverted microscope (Carl Zeiss, Jena, Germany). Force measurements were recorded at room temperature in PBS and finally all SCFS data were analyzed using SPIP software (Image Metrology A/S, Hørsholm, Denmark).

"Long term adhesion protocol"
The cantilever approached a selected bacterial cell with a set point of 5 nN, followed by a pause of 5 s with force feedback on, to apply underpressure (~100 kPa) to reversibly immobilize the cell at the pyramidal opening. While the probe with the attached cell was retracted at a piezo velocity of 1 µm s^{-1}, forces were recorded. Underpressure was maintained during this process until the bacterium was completely detached from the substrate. Subsequently the bacterium was released from the cantilever using an overpressure pulse of ~100 kPa. The cells were allowed to sediment and attach to the surface for two hours before SCFS experiments were started. Using this approach one force-distance (F–d) curve was recorded per cell. For measurements of *E. coli*-PDA interactions, cantilevers with a spring constant of approximately 2.5 N m^{-1} were used, whereas for *E. coli*-glass interactions 0.2 N m^{-1} cantilevers were used.

"Cell probe protocol"
In experiments where the cells were initially not attached to a substrate, an individual, floating bacterial cell was aspirated along the aperture directly from solution using ~100 kPa underpressure, and the cell was used throughout the experiment as a cell probe. After all desired measurements (more than one F-d curve per bacterium), the cell was released by a ~100 kPa overpressure pulse, and the cantilever was ready for use with another bacterial cell. The cell probe was used to approach the substrate with a set point between 1 and 100 nN (as stated in results), followed by a pause of 0-240 s, with force feedback on and a piezo velocity of 1 µm s^{-1}. For all experiments performed with *E. coli* cantilevers with a spring constant of approximately 0.2 N m^{-1} were used, whereas SCFS experiments with *S. pyogenes* were performed with ~2.5 N m^{-1} cantilevers.

3. Results

3.1. Instrument development for bacterial adhesion experiments

To establish a broadly applicable protocol to quantify the adhesion forces of bacterial cells using reversible fixation to the cantilever by means of FluidFM, several challenges needed to be overcome. In particular, these obstacles relate to the small size of bacteria (usually 0.5 to 5 µm) and the variation in morphology (usually rods or spheres). Cantilevers with a closed pyramidal tip were taken as a starting point to establish bacterial adhesion measurements with FluidFM. To adapt the pyramidal tip probes, a focused ion beam (FIB) was used. The pyramid apex was sloped to compensate for the 10° tilt angle of the AFM probe holder (Figure 1 B, C[28]), and circular openings with diameters from 300 to 900 nm were drilled in the cut pyramidal apex (Figure 1 D). The tip was designed to allow for defined openings parallel to the substrate, preventing unwanted direct pyramid substrate contact and ensuring that only one cell was immobilized at the cantilever opening at a time (Figure 1 D). Furthermore, a hemi-cylindrical design of the pyramidal opening (Figure 1 E) was generated. After verifying the suitability of both probe designs for bacterial adhesion measurements, we continued to work with probes having a round aperture at the apex because of the less labor- and cost-intensive production process. While for cocci and rod shaped bacteria the circular design is adequate, the hemi-cylindrical probe design highlights the potential of FIB-based probe adaptations for the investigation of specific cell morphologies.
Because cell immobilization at the cantilever aperture depends on the applied underpressure and the size of the opening, maximal forces (F_{max}) were estimated using the formula $F_{max} = p\pi r^2$, where p corresponds to the underpressure in Pa, and r corresponds to the radius of the opening in m. Using this approximation, the estimated maximal forces were 64 nN for an underpressure of 100 kPa and a 900 nm pyramidal opening. Nonetheless, a compromise had to be found between the maximization of the opening size and the formation of a tight seal between the bacterium and the aperture: when the cantilever approaches the cell, the size of the bacterial cell must be greater than the aperture edge to exploit the suction force.
An additional factor in the establishment of bacterial adhesion measurements is cantilever stiffness. The first pyramidal FluidFM probes were characterized by a spring constant of approximately 2.5 N m^{-1}.[29] These cantilevers are suitable for measuring adhesion forces of 1 nN or higher; however, lower adhesion forces will be important depending on the substrate and cell type that are measured. The rather stiff cantilevers would result in a too high noise; thus, we also used cantilevers with a lower spring constant. Reducing the channel thickness from 1 to 0.2 µm decreased the spring constant by an order of magnitude to approximately 0.2 N m^{-1}; the channel was still framed by 250 nm thick cantilever walls.

3.2. *Escherichia coli* long-term adhesion force quantification

To test SCFS using reversible cell immobilization onto the pyramidal aperture via underpressure, we used the model bacterium *E. coli*. In a first set of experiments, the bacterial adhesion was measured after more than two hours of unperturbed incubation time on two different surfaces. We used glass and polydopamine (PDA)-coated substrates. PDA is inspired by the 3,-4-dihydroxy-L-phenylalanine secreted from mussels[13, 19, 22, 30] and is considered the most efficient wet adhesive for immobilizing a cell onto the cantilever used in conventional AFM. Here, we wanted to use PDA as a

benchmark for the FluidFM approach to examine whether cells can be detached from a PDA-coated substrate.

The bacteria were allowed to sediment and attach to the chosen substrates before the force spectroscopy experiments were performed. Then, the cantilever approached an adherent cell, which was optically chosen under the fluorescence microscope, with a preselected force setpoint (Figure 1 A, 2 A). During a 5 s pause, underpressure (~ -100 kPa) was applied to immobilize the cell on the cantilever opening before the cantilever, together with the cell, was retracted (Figure 1 A, 2 A). After the cell was completely detached from the substrate, an overpressure pulse (~ +100 kPa) was used to release the cell from the cantilever. Indeed, the cells could be detached from both substrates, i.e., glass and the PDA-coated surfaces. Microchanneled probes with a pyramid with a circular opening of approximately 900 nm and a spring constant of ~ 2.5 N m^{-1} allowed the quantification of the adhesion forces of *E. coli* cells that adhered to PDA with an average force of 4-8 nN (Figure 3 A); even higher forces up to 14 nN was also measured for some cells, demonstrating the biological cell variability in bacterial populations (n = 25 cells). Notably, a long detachment distance of approximately 750 nm (Figure 3 B) was required for cell detachment; this distance is consistent with that of other studies, where comparable distances were observed and were related to cell deformation, cell appendages or the stretching of cell surface polymers that interact with the substrate.[31, 32] These measurements of *E. coli* on PDA showed a peak-to-peak noise of approximately 250 pN (rms: 230 pN) (Figure 3 B), which was qualitatively high enough. However, softer probes (0.2 N m^{-1}) with an improved signal-to-noise ratio and thus a peak-to-peak noise of 20 pN (rms: 12 pN) (Figure 3 C) were required to measure the adhesion forces of *E. coli* on glass, where an average adhesion force of 1.8 nN was measured (n = 10 cells).

Because chemical cell immobilization occasionally leads to cell inactivation[22], the cell survival after SCFS using FluidFM was checked. Exploiting the reversibility of the immobilization-release process with the FluidFM, the bacteria were deposited back onto the substrate after SCFS. Subsequently, cell division was indeed observed, showing cell survival (Figure 2 B).

3.3. *E. coli* adhesion versus contact time and force setpoint on different substrates

As an alternative to the detachment of cells already adhered to a substrate, it is also possible to aspirate a floating cell in solution against the apex aperture and perform force spectroscopy with the cell fixed to the probe. Taking advantage of this approach, we investigated the nonspecific, electrostatic interactions of *E. coli* on glass and poly-$_L$-lysine (PLL) as a function of the contact time (Figure 4 A, B). Electrostatic interactions between PLL and bacteria, similar to those between PDA and bacteria, are also commonly used for cell immobilization on the cantilever in conventional AFM experiments.[17] Low stiffness probes allowed us to measure forces of approximately 120 pN after a contact of 2 s, while increasing the interaction time to 60 s or more between bacterial cells and glass led to stronger interaction forces of up to 500 pN (Figure 4 A). As expected, the adhesion forces on PLL also became stronger in the first 60 s, as was shown for *E. coli* on glass; while overall, higher forces were recorded on PLL than on glass. The forces increased from approximately 2 nN after 2 s up to 4 nN after 60 s (with a setpoint of 1 nN as was used for glass) (Figure 4 A, B). Because the order of the measurements did not influence the measured forces or detachment distances during replicate measurements of individual cells, no evidence for a cell surface alteration after PLL contact and underpressure application was obtained. This observation is based on the force distance curves of *E. coli* on PLL, which show a similar pattern for three replicate measurements for different contact times (Figure 4 C).

In addition to longer contact times, higher setpoints also resulted in stronger adhesion forces to PLL. A twenty-time higher setpoint led to approximately three-times higher forces. The adhesion forces increased from 4 to 14 nN as the setpoint increased from 1 to 20 nN with a constant contact time of 60 s (Figure 4 B). Higher setpoints can be expected to generate tighter cell substrate contact, thus explaining the higher interaction forces. Additionally, vertical compression of the cells increases with higher setpoints (Figure 4 D). The vertical compression was extracted from the forward force spectroscopy curves as the distance between the contact point and the distance at which the setpoint is reached, corrected for cantilever deflection. Stronger cell compression is accompanied by cell stretching and deformation, often leading to a larger contact area of the cell and resulting in stronger adhesion forces. The nonlinear increase in the cell compression with increasing setpoint can be approximated by the Hertz model, which describes the contact mechanics of elastic materials.[33, 34]

In addition to the increase in adhesion force with time and setpoint, the distance required to detach a bacterial cell from the substrate also correlated positively with these two parameters (Figure S 1 A). At a setpoint of 20 nN and contact times longer than 10 s, the detachment distances became as long as 4 µm, which was discernable in the detachment curves as long force plateaus following the main adhesion peak and ending with a force jump in the pN range (Figure 4 C, E). For force spectroscopy measurements with setpoints smaller than 20 nN, detachment distances of maximal 300 nm were recorded, and no force plateaus occurred (Figure 4 C). For those SCFS experiments, the measured adhesion forces linearly correlated with the detachment distance and the performed detachment work (Figure S 1 A, B), as previously shown for yeast cells.[25] Detachment work refers to the complete detachment of the cell from the substrate and is determined from the area between the retraction force curve and the baseline; this measure is significantly influenced by the adhesive effect of cell appendages and cell deformation during cantilever retraction. Bacterial cells were more strongly compressed during the approaches with higher setpoints (Figure 4 D); therefore, a stronger cell deformation, and thus more detachment work, is required during cell detachment. This requirements explains the loss of force-distance correlation for higher setpoints and for longer contact times. With this "cell probe" protocol, i.e., using the same cell for consecutive adhesion measurements,

numerous force spectroscopy measurements were performed (up to 110 in our set up) with the same cell probe. The very same cantilever could subsequently still be used to measure different cells in series, here, *E. coli* cells on glass surfaces (n=17) and on PLL (n=16) coated glass. The throughput that could be achieved with a single cantilever also revealed that different cells showed similar behavior regarding setpoint and contact time dependence. Furthermore measured forces of different cells under the same conditions lay in a comparable range: for example an average adhesion force of 110 ±56 pN were measured for *E.coli*-glass interactions after 5 s contact time.

3.4. *Streptococcus pyogenes* adhesion force quantification: from single-cell to cell chain detachment

Because bacteria are morphologically diverse, we aimed at validating the FluidFM-based SCFS procedures introduced above, with the smaller, spherically shaped *S. pyogenes*; to the best of our knowledge, *S. pyogenes* has not been measured with conventional AFM before. *S. pyogenes* is a Gram positive human pathogen that causes superficial skin and severe systemic infections, resulting in approximately 500 000 deaths worldwide each year. [35] Attachment to host tissue is the initial step of infection that is often followed by biofilm formation, highlighting the importance of gaining more insight into the adhesion process. Initially, the above established cell probe protocol, which involves the aspiration of a swimming cell and SCFS measurements, was validated for *S. pyogenes* on glass. The adhesion forces increased from 3 nN at setpoints of 5 nN up to approximately 14 nN at a setpoint of 100 nN (Figure 5 A). The recorded forces were approximately ten times higher than the forces measured for the *E. coli*-glass interactions, whereas the *E. coli*-PLL interactions were in a comparable range (Figure 4 B, 5 A). As shown for *E.coli* on PLL, the vertical cell compression increased in a nonlinear manner with rising setpoints (Figure 5 B). Comparison of these data revealed that stronger forces were required to compress *S. pyogenes* than for *E. coli* cells. For *E. coli*, 10 nN was sufficient to compress the cell approximately 80 nm, whereas for *S. pyogenes*, approximately 80 nN was required for the same cell compression.

Naturally, *S. pyogenes* mainly occurs in cell chains (Figure 5 C), making it difficult to use FluidFM for multiple cell detachments in a row with simultaneous force recording. Because the cell probe approach is not suitable for this task, we used the cantilever to approach the outermost adherent cell of a chain, and up to four bacteria were sequentially detached from the glass (Figure 5 C and Video S 1). In the backward force curve, zipper-like detachment behavior was recorded. The curve lacked a major adhesion peak but did contain several smaller peaks; in total these peaks correspond to a complete detachment force of approximately 35 nN for four cells (Figure 5 D). The overall detachment distance agreed with the length of the detached cell chain (Figure 5 C, D). Sequential cell detachment occurred until the bacteria-glass interactions became too strong or the maximal probe retraction was achieved due to the available piezo range (10 µm). As the cells were detached from the substrate, the connection between the cells needed to be stronger than the cell-substrate interactions.

4. Discussion

In this study, we established SCFS for bacterial adhesion force quantification using FluidFM. The approach enables bacterial cell adhesion measurements for contact times of more than 2 hours using glass and surfaces coated with strong adhesives without additional chemical or physical perturbation by the cantilever during the cell-substrate contact. While in previous studies PDA or PLL were used to fix the cell to the AFM cantilever disregard changes of the cell potentially triggered by these polymers, in this study specifically *E. coli*- PDA and PLL interactions were measured. Thus far, most AFM-based SCFS measurements have recorded interaction forces after a maximum of 60 s[17] and were limited to forces lower than PDA adhesion forces because the latter or compounds with similar properties were used for cell immobilization to the cantilever. Furthermore, the reversible cell immobilization on the cantilever allowed to use a single probe for serial measurements of many bacterial cells, enabling direct comparison of cell to cell variations.

Together with the probe design optimization for the desired opening size, the spring constant shift to 0.2 N m^{-1} permits measurements of bacterial adhesion forces down to 20 pN. Consequently, in addition to allowing measurements of adhesion forces in the low pN range, which are relevant for bacterial adhesion, this technique can also measure the detachment force patterns in retraction curves. For example, long force plateaus followed by jumps in the pN range became visible. Detachment curves most likely have specific characteristics, such as those seen for *E. coli*-PLL interactions, due to cell appendages such as pili. Similar patterns were visible for *E. coli* on aminosilane, which possesses surface chemistry characteristics comparable to those of PLL; these force patterns were attributed to pili-mediated adhesion.[32] The pili associated adhesion of *Pseudomonas aeruginosa* to abiotic substrates also showed similar force patterns with plateaus followed by jumps in the same force range of 200 pN.[36] On glass and PLL, bond strengthening occurred within the first 2 minutes for both *E. coli* and *S. pyogenes*. Previous studies have suggested that during experiments with contact times up to several minutes, bacteria eliminate excessive water in between the cell and the substrate, allowing for a tighter contact that facilitates the formation of more contact points and thus strengths the adhesion.[4, 37] Comparable time-dependent bond strengthening of nonspecific interactions was shown for oral bacteria on bovine serum albumin.[38] In addition to contact time-dependent bond strengthening, setpoint-dependent bond strengthening was shown for *E. coli* and *S. pyogenes*. A higher setpoint correlates with a stronger vertical cell compression. While Elter et al. showed increased vertical cell compression of fibroblasts with higher setpoints,[33] Chen et al. linked stronger bacterial cell wall deformation to higher adhesion forces.[39]

S. pyogenes requires higher setpoints to be compressed to the same extent as *E. coli*. These data are in line with those of an earlier AFM study in which the cell stiffness of Gram negative (*E. coli*) and Gram positive (*B. subtilis*) bacteria were measured, revealing that the Gram positive bacteria are stiffer than Gram negative bacteria.[40] While the Gram negative *E. coli* only has a thin peptidoglycan layer, the Gram positive *S. pyogenes* possess a thick and rigid layer and it was proposed that the degree of elasticity is related to the properties of their respective peptidoglycan layers.[40] These differences in cell architecture might explain the variances in vertical cell compression shown here.

In addition to adhesion forces, the required detachment distance increased with the setpoint and contact time. On the one hand, stronger adhesion allows for more cell stretching before the final PLL-cell connection is ruptured. On the other hand, additional cell surface structures that mediate bacterial adhesion most likely come into play at higher setpoints and longer contact times.

Generally, comparing the adhesion forces recorded by AFM in different studies is a delicate task, because the measured forces strongly depend on the parameters used for SCFS, such as the setpoint and contact time, as shown in this study. Zeng et al. performed SCFS using conventional AFM with *E. coli* on glass.[31] We have measured forces in a comparable range of approximately 100 pN using the same setpoint and contact time as those of the Zeng study.[31] Hence, reversible immobilization using underpressure or irreversible immobilization using Cell-Tak (a wet adhesive comparable to PDA) led to similar results, suggesting no effect of the immobilization method. In other studies Cell-Tak, PLL or PDA were used to immobilize cells onto the cantilever;[13, 17, 39] thus, adhesion forces stronger than the ones exerted by these polymers could not be measured up to now. Only lateral detachment forces of *E. coli* on PLL were measured; these forces were approximately 0.7 nN, which is in the same order of magnitude as the forces measured in this study. Due to the lateral detachment, the forces are not directly comparable to the perpendicular forces measured using FluidFM.[41] Overall, so far only a few AFM SCFS studies have been performed with bacterial cells. Most prominent investigations of *Staphylococci* revealed interactions with abiotic and biotic yeast surfaces in the range of hundreds of pN up to a few nN.[17, 30, 42, 43] In all studies, the forces were measured after contact times of a few ms up to a maximum of 60 s, whereas the FluidFM technology provided the first force measurements after more than two hours of unperturbed contact time.

5. Conclusion and Outlook

In this manuscript, we introduced a protocol for measuring the adhesion forces of living single bacterial cells using FluidFM technology. After adapting the probe design, especially by increasing the cantilever sensitivity, detachment forces in ranges of a few pN to tens of nN were measured, and the force patterns in retraction curves were resolved. For SCFS, the hollow cantilever was either directed to approach already attached cells after hours of substrate contact or floating cells were aspirated along the pyramidal aperture to generate a cell probe for dynamic SCFS experiments. The experimental approaches show the versatility of the FluidFM technology for adhesion measurements after contact times as short as seconds but also as long as hours without cell perturbation. In addition to providing longer contact times, the reversible cell immobilization on the cantilever by underpressure allows for measurements of more than one cell using a single probe. Thus, time-consuming cantilever calibration and cell probe preparation, which are required for conventional AFM, are avoided. Bacterial SCFS was demonstrated using bacteria of different shapes and surface properties; the Gram negative model organism *E. coli* and the Gram positive *S. pyogenes*. Moreover, cell groups were separated from glass, and this separation revealed distinct adhesion patterns in the detachment curve due to the sequential cell detachment. Therefore, the FluidFM technology provides a platform for investigating bacterial adhesion. Future applications may involve quantifying the forces of various bacterial strains with different surface properties or investigating the adhesion to different substrates; these substrates may range from abiotic substrates to cell-to-cell interactions, such as those in biofilm formation or mammalian cell infection.

Acknowledgements

This work was supported by the Swiss innovation promotion agency KTI-CTI (11722.1 PFNM-NM) (to JAV and TZ) and a grant from the Swiss National Science foundation (SNSF) (to TZ). The authors thank Patrick Frederix (Nanosurf AG, CH), Edin Sarajlic (SmartTip BV, NED), Michael Gabi, Pascal Behr and Pablo Dörig (Cytosurge AG, CH) for support, Jérôme Polesel Maris (TEFAL Groupe SEB SA, France) and Orane Guillaume-Gentil for discussions and reading of the manuscript, Federica Andreoni and Annelies Zinkernagel (University of Zurich) for the *S. pyogenes* strain and their support.

Notes and references

[a]Institute of Microbiology, ETH Zurich, Vladimir-Prelog-Weg 4, 8093 Zurich, Switzerland

[b]Laboratory of Biosensors and Bioelectronics, Institute for Biomedical Engineering, ETH Zurich, Gloriastrasse 35, 8092 Zurich, Switzerland

E-mail: zambelli@biomed.ee.ethz.ch; vorholt@micro.biol.ethz.ch

Electronic Supplementary Information (ESI) available: [Video S1. Detachment of a *S. pyogenes* cell chain from glass substrate. The cantilever is approached on the outermost adherent cell of a chain and four bacteria were then sequentially detached. The sequential cell detachment suddenly stopped after four bacteria. This possibly occurred because bacteria-glass interactions became too strong or the maximal probe retraction was reached. The cells spontaneously detached from the cantilever flipping back on the surface. Figure S1. A) Adhesion force–distance and B) adhesion force-detaching work correlation of *E.coli* on

PLL for setpoints of 1 and 10 nN. Circle: 1 nN setpoint, square: 10 nN.].
See DOI: 10.1039/b000000x/

1 W. M. Dunne, Jr., *Clin Microbiol Rev*, 2002, **15**, 155-166.
2 L. Hall-Stoodley, J. W. Costerton and P. Stoodley, *Nat Rev Microbiol*, 2004, **2**, 95-108.
3 G. Li, P. J. Brown, J. X. Tang, J. Xu, E. M. Quardokus, C. Fuqua and Y. V. Brun, *Mol Microbiol*, 2012, **83**, 41-51.
4 H. J. Busscher and A. H. Weerkamp, *FEMS microbiology letters*, 1987, **46**, 165-173.
5 M. Katsikogianni and Y. F. Missirlis, *Eur Cell Mater*, 2004, **8**, 37-57.
6 Y. Wang, R. Narain and Y. Liu, *Langmuir*, 2014, **30**, 7377-7387.
7 W. R. Bowen, A. S. Fenton, R. W. Lovitt and C. J. Wright, *Biotechnology and bioengineering*, 2002, **79**, 170-179.
8 M. R. Nejadnik, H. C. van der Mei, W. Norde and H. J. Busscher, *Biomaterials*, 2008, **29**, 4117-4121.
9 G. Binnig, C. F. Quate and C. Gerber, *Physical review letters*, 1986, **56**, 930-933.
10 Y. F. Dufrene, *Nat Rev Microbiol*, 2008, **6**, 674-680.
11 J. Helenius, C. P. Heisenberg, H. E. Gaub and D. J. Muller, *J Cell Sci*, 2008, **121**, 1785-1791.
12 Y. Dufrêne, *Curr Opin Microbiol*, 2003, **6**, 317-323.
13 A. Beaussart, S. El-Kirat-Chatel, R. M. Sullan, D. Alsteens, P. Herman, S. Derclaye and Y. F. Dufrene, *Nat Protoc*, 2014, **9**, 1049-1055.
14 A. M. Baró and R. G. Reifenberger, *Atomic force microscopy in liquid: Biological applications*, Wiley-VCH Verlag GmbH & Co. KGaA, 1 edn., 2012.
15 D. J. Muller, M. Krieg, D. Alsteens and Y. F. Dufrene, *Curr Opin Biotechnol*, 2009, **20**, 4-13.
16 M. Benoit and H. E. Gaub, *Cells Tissues Organs*, 2002, **172**, 174-189.
17 E. S. Ovchinnikova, B. P. Krom, H. C. van der Mei and H. J. Busscher, *Soft Matter*, 2012, **8**, 6454-6461.
18 D. T. Le, Y. Guerardel, P. Loubiere, M. Mercier-Bonin and E. Dague, *Biophys J*, 2011, **101**, 2843-2853.
19 J. M. Thwala, M. Li, M. C. Wong, S. Kang, E. M. Hoek and B. B. Mamba, *Langmuir*, 2013, **29**, 13773-13782.
20 R. J. t. Emerson, T. S. Bergstrom, Y. Liu, E. R. Soto, C. A. Brown, W. G. McGimpsey and T. A. Camesano, *Langmuir*, 2006, **22**, 11311-11321.
21 A. Beaussart, S. El-Kirat-Chatel, P. Herman, D. Alsteens, J. Mahillon, P. Hols and Y. F. Dufrene, *Biophys J*, 2013, **104**, 1886-1892.
22 S. Kang and M. Elimelech, *Langmuir*, 2009, **25**, 9656-9659.
23 A. Meister, M. Gabi, P. Behr, P. Studer, J. Voros, P. Niedermann, J. Bitterli, J. Polesel-Maris, M. Liley, H. Heinzelmann and T. Zambelli, *Nano Lett*, 2009, **9**, 2501-2507.
24 O. Guillaume-Gentil, E. Potthoff, D. Ossola, C. M. Franz, T. Zambelli and J. A. Vorholt, *Trends in biotechnology*, 2014, **32**, 381-388.
25 E. Potthoff, O. Guillaume-Gentil, D. Ossola, J. Polesel-Maris, S. LeibundGut-Landmann, T. Zambelli and J. A. Vorholt, *Plos One*, 2012, **7**, e52712.
26 P. Dorig, P. Stiefel, P. Behr, E. Sarajlic, D. Bijl, M. Gabi, J. Voros, J. A. Vorholt and T. Zambelli, *Appl Phys Lett*, 2010, **97**, 023701.
27 S. Chatellier, N. Ihendyane, R. G. Kansal, F. Khambaty, H. Basma, A. Norrby-Teglund, D. E. Low, A. McGeer and M. Kotb, *Infect Immun*, 2000, **68**, 3523-3534.
28 R. R. Gruter, J. Voros and T. Zambelli, *Nanoscale*, 2013, **5**, 1097-1104.
29 O. Guillaume-Gentil, E. Potthoff, D. Ossola, P. Dorig, T. Zambelli and J. A. Vorholt, *Small*, 2013, **9**, 1904-1907.
30 P. Loskill, H. Hahl, N. Thewes, C. T. Kreis, M. Bischoff, M. Herrmann and K. Jacobs, *Langmuir*, 2012, **28**, 7242-7248.
31 G. Zeng, T. Muller and R. L. Meyer, *Langmuir*, 2014, **30**, 4019-4025.
32 H. Xu, A. E. Murdaugh, W. Chen, K. E. Aidala, M. A. Ferguson, E. M. Spain and M. E. Nunez, *Langmuir*, 2013, **29**, 3000-3011.
33 P. Elter, T. Weihe, R. Lange, J. Gimsa and U. Beck, *European biophysics journal : EBJ*, 2011, **40**, 317-327.
34 H. Hertz, *Journal für die reine angewandte Mathematik*, 1881, **92**, 156-171.
35 J. R. Carapetis, A. C. Steer, E. K. Mulholland and M. Weber, *The Lancet. Infectious diseases*, 2005, **5**, 685-694.
36 A. Beaussart, A. E. Baker, S. L. Kuchma, S. El-Kirat-Chatel, G. A. O'Toole and Y. F. Dufrene, *ACS Nano*, 2014, DOI: 10.1021/nn5044383, DOI: 10.1021/nn5044383.
37 J. Li, H. J. Busscher, J. J. Swartjes, Y. Chen, A. K. Harapanahalli, W. Norde, H. C. van der Mei and J. Sjollema, *Soft Matter*, 2014, **10**, 7638-7646.
38 H. C. van der Mei, M. Rustema-Abbing, J. de Vries and H. J. Busscher, *Appl Environ Microbiol*, 2008, **74**, 5511-5515.
39 Y. Chen, A. K. Harapanahalli, H. J. Busscher, W. Norde and H. C. van der Mei, *Appl Environ Microbiol*, 2014, **80**, 637-643.
40 V. Vadillo-Rodriguez, S. R. Schooling and J. R. Dutcher, *J Bacteriol*, 2009, **191**, 5518-5525.
41 T. Zhang, Y. Q. Chao, K. M. Shih, X. Y. Li and H. H. P. Fang, *Ultramicroscopy*, 2011, **111**, 131-139.
42 P. Herman, S. El-Kirat-Chatel, A. Beaussart, J. A. Geoghegan, T. Vanzieleghem, T. J. Foster, P. Hols, J. Mahillon and Y. F. Dufrene, *Langmuir*, 2013, **29**, 13018-13022.
43 A. Beaussart, P. Herman, S. El-Kirat-Chatel, P. N. Lipke, S. Kucharikova, P. Van Dijck and Y. F. Dufrene, *Nanoscale*, 2013, **5**, 10894-10900.
44 B. Cormack, *Curr Opin Microbiol*, 1998, **1**, 406-410.
45 X. Lauth, M. von Kockritz-Blickwede, C. W. McNamara, S. Myskowski, A. S. Zinkernagel, B. Beall, P. Ghosh, R. L. Gallo and V. Nizet, *Journal of innate immunity*, 2009, **1**, 202-214.
46 J. Sambrook, Fritsch, E. F., Maniatis, T., *Molecular cloning: A laboratory Manual*, Cold Spring Harbor Lab. Press, Plainview, NY, 2nd edn., 1989.
47 N. P. Huang, R. Michel, J. Voros, M. Textor, R. Hofer, A. Rossi, D. L. Elbert, J. A. Hubbell and N. D. Spencer, *Langmuir*, 2001, **17**, 489-498.
48 J. E. Sader, J. W. M. Chon and P. Mulvaney, *Rev Sci Instrum*, 1999, **70**, 3967-3969.

Figure Legends

Figure 1. FluidFM-based single-cell force spectroscopy. A) Simplified schematic view of SCFS using FluidFM in liquid. The black arrows correspond to the forward and backward movement of the probe, and the blue arrows indicate the applied under– and overpressure. B) Pyramids were sloped with a 10° angle prior to the milling of the opening using focused ion beam (FIB). C) Scanning electron microscopy (SEM) image of a cantilever with a closed pyramidal tip. Scale bar corresponds to 10 µm. D and E) SEM images of the tip of a microchanneled cantilever for fluidic force microscopy. D) 900 nm opening achieved by FIB treatment perpendicular to the substrate. E) Side view of a pyramid with a hemi-cylindrical aperture design, achieved by FIB treatment parallel to the substrate. The scale bars correspond to 1 µm.

Figure 2. FluidFM-based single-cell force spectroscopy. A) Optical microscope images of the experimental principle. Optical targeting of an *E. coli* cell on polydopamine and immobilization to the cantilever through the application of under pressure followed by single-cell force spectroscopy (SCFS) measurement and the subsequent release of the measured cell (indicated by green boarder arrow). The scale bar corresponds to 10 µm. B) Cell division after SFCS and reattachment of the cell of interest, indicated by a red boarder, on polydopamine. The scale bar corresponds to 5 µm.

Figure 3. Bacterial adhesion on abiotic surfaces. A) Adhesion force histogram obtained from the SCFS measurements of *E. coli* cells on polydopamine (n= 25 cells). Representative force distance curves of *E. coli* on B) polydopamine obtained using a cantilever with a spring constant of ~2.5 N m^{-1} or on C) glass using a cantilever with a spring constant of ~0.2 N m^{-1}.

Figure 4. *E. coli* adhesion on abiotic substrates. The adhesion forces on A) glass and B) poly-L-lysine (PLL) depend on the contact time. All measurements on glass were performed with a setpoint of 1nN. B) The PLL interaction forces also depend on the applied force setpoint during the approach. Squares: 1 nN setpoint, circle: 10 nN setpoint, triangle: 20 nN setpoint. C) Representative force distance curves of *E. coli* on PLL for approaches with a setpoint of 1 nN. The violet curves correspond to a contact time of 0 s, and the black curves correspond to a contact time of 60 s. D) The vertical cell compression of *E. coli* on PLL depends on the applied setpoint during the approach curve for a constant contact time of 5 s. E) Representative detail of the force distance curves of *E. coli* on PLL for a 20 nN setpoint and 30 s of contact time, showing force plateaus that lead to detachment distances up to 1.3 µm.

Figure 5. *S. pyogenes* detachment from glass. A) The measured adhesion forces of *S. pyogenes* on glass depend on the setpoint at a constant contact time of 10 s. B) The vertical compression of the cell during approach depends on the defined setpoint. C) Optical microscopy image of *S. pyogenes* cell chains on glass. The cantilever is approaching the outermost cell of the chain. Scale bar corresponds to 5 µm. D) Representative retraction force curve of the detachment event of four connected cells shown in C).

Abstract for the table of contents entry

Achieving higher immobilization forces than the state-of-the-art cell-cantilever binding in single-cell force spectroscopy, by using fluidic force microscopy, demonstrates the potential to quantify bacterial adhesion. Reversible cell fixation on the pyramidal tip allows for adhesion measurements in the nN range in a serial manner for many bacterial cells with a single cantilever.

Figure S1. A) Adhesion force–distance and B) adhesion force-detaching work correlation of *E.coli* on PLL for setpoints of 1 and 10 nN. Circle: 1 nN setpoint, square: 10nN.

Video S1. Detachment of a *S. pyogenes* cell chain from the glass substrate. The cantilever is approached on the outermost adherent cell of a chain and four bacteria were then sequentially detached. The sequential cell detachment suddenly stopped after four bacteria. This possibly occurred because bacteria-glass interactions became too strong or the maximal probe retraction was reached. The cells spontaneously detached from the cantilever flipping back on the surface.

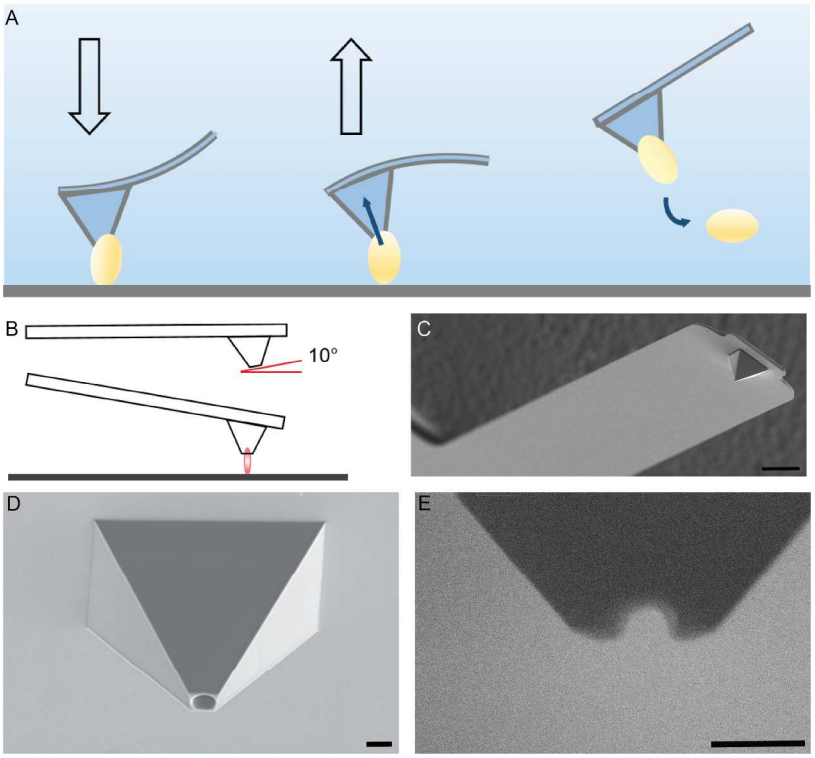

210x161mm (300 x 300 DPI)

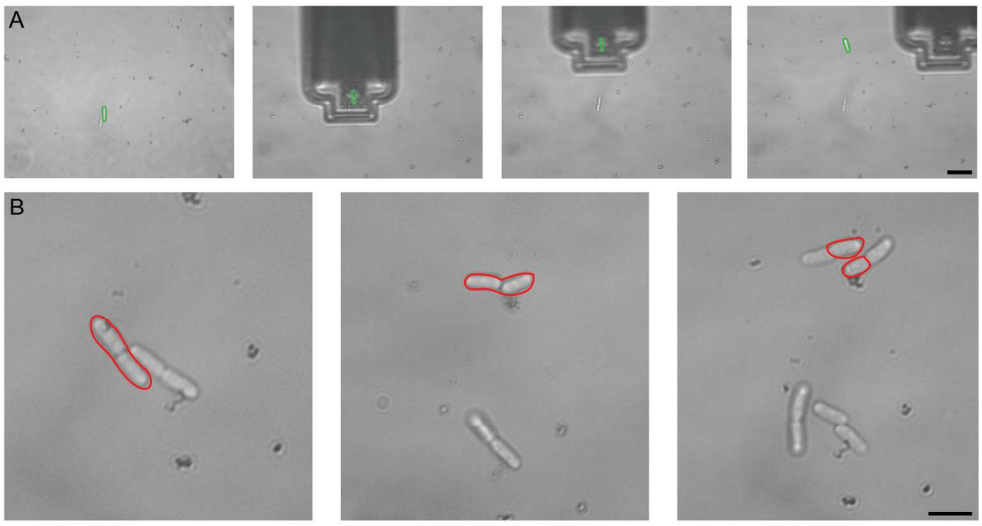

182x97mm (300 x 300 DPI)

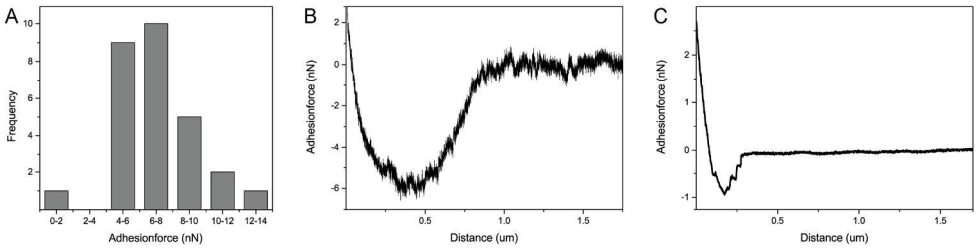

210x54mm (300 x 300 DPI)

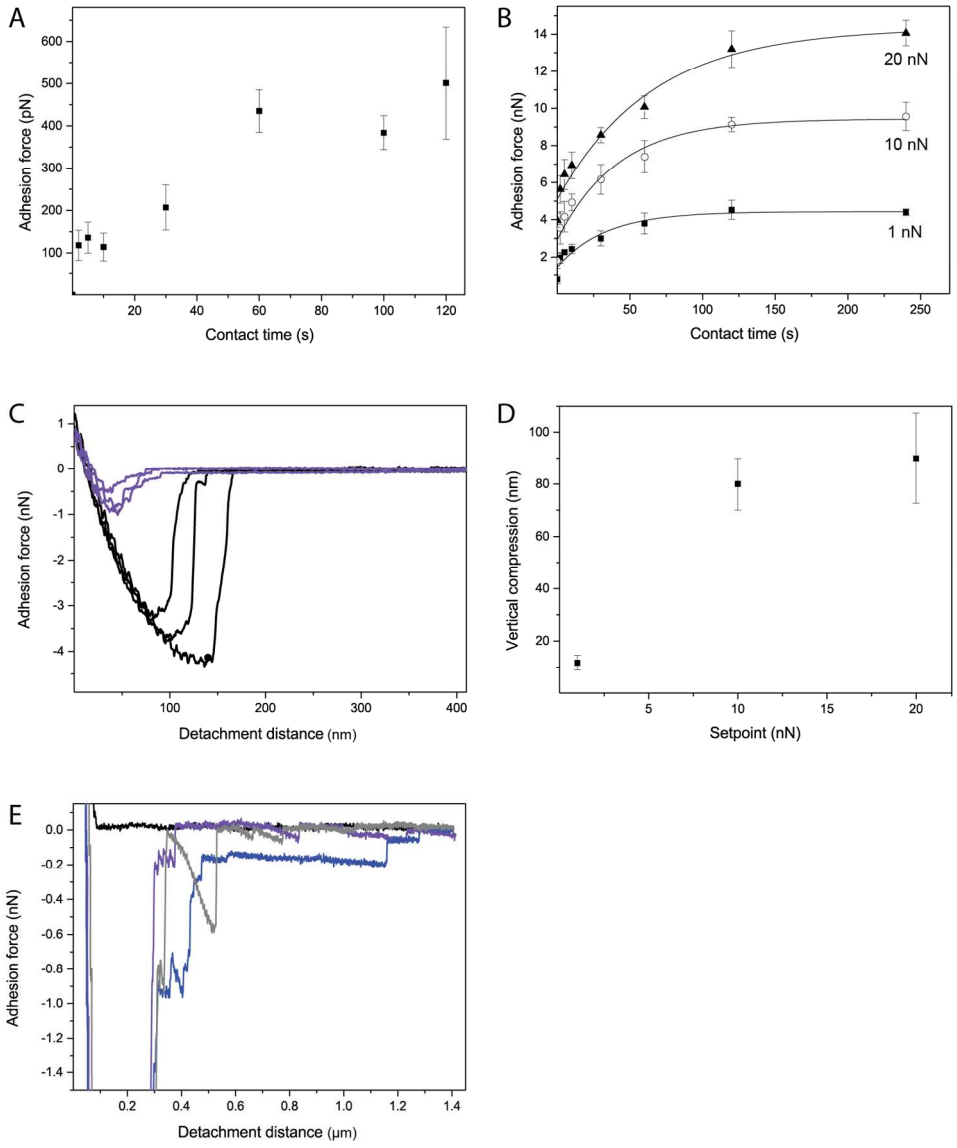

148x177mm (300 x 300 DPI)

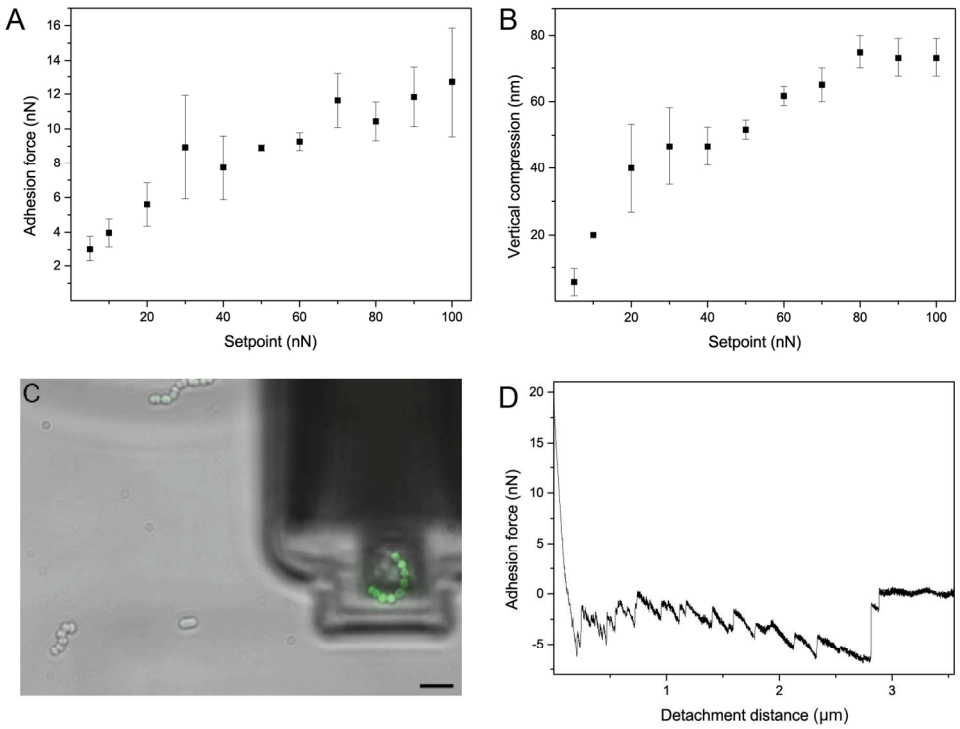

145x112mm (300 x 300 DPI)